International Conference on Space Optics—ICSO 2004

Toulouse, France

30 March–2 April 2004
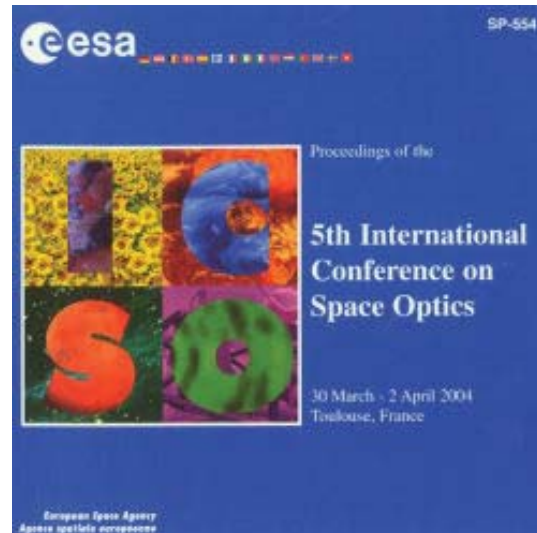
Low-cost thermal-IR imager for an Earth observation microsatellite

Brian D. Oelrich, Craig I. Underwood

LOW-COST THERMAL-IR IMAGER
FOR AN EARTH OBSERVATION MICROSATELLITE

Brian D. Oelrich[(1)], Dr. Craig I. Underwood[(1)]

[(1)]*Surrey Space Centre, University of Surrey, Guildford, Surrey, GU2 7XH, UK, E-mail: B.Oelrich@sstl.co.uk*

ABSTRACT

A new class of thermal infrared (TIR) Earth Observation (EO) data will become available with the flight of miniature TIR EO instruments in a multiple micro-satellite constellation. This data set will provide a unique service for those wishing to analyse trends or rapidly detect anomalous changes in the TIR characteristics of the Earth's surface or atmosphere (e.g. fire detection). Following a preliminary study of potential mission applications, uncooled commercial-off-the-shelf (COTS) technology was selected to form the basis of a low-cost, compact instrument capable of complementing existing visible and near IR EO capabilities on a sub-100kg Surrey micro-satellite. The preliminary 2-3 kg instrument concept has been designed to yield a 325 m ground sample distance over a 200 km swath width from a constellation altitude of 700 km. The radiometric performance, enhanced with time-delayed integration (TDI), is expected to yield a NETD less than 0.5 K for a 300 K ground scene. Fabrication and characterization of a space-ready instrument is planned for late 2004.

1. INTRODUCTION

The role of space-based Earth Observation (EO) in the thermal infrared (TIR) waveband (8 to 12 µm) has been well demonstrated over the years by numerous missions such as AASTR [1], MODIS [2], BIRD [3], and ETM+ [4]. The user community for such data products is well served and is likely to become more so with further enhancements in (1) radiometric sensitivity or noise equivalent temperature difference (NETD), (2) spatial resolution or ground sample distance (GSD), and (3) ground coverage (revisit time). However, because of the large mission costs and the finite limits of optics size in space, TIR instrument developers typically have to make concessions in one of these factors (GSD, NETD, or revisit time) in order to optimise the other two. As a result, two general classes of TIR EO instruments have emerged as illustrated in Fig. 1. Group 1 is dominated by instruments optimising NETD and spatial resolution at the cost of a decreased revisit time and group 2 is dominated by instruments optimising NETD and ground coverage (revisit time) at the expense of GSD.

This paper proposes a departure from traditional TIR instrument advancement by exploiting the unique capabilities of low-cost EO micro-satellite constellations. Because small EO satellites are limited in their ability to compete directly with existing, larger platforms, they tend to focus instead on reducing the costs of data products or providing niche services currently ill-served. For example, in the visible and near infrared (NIR) wavebands, the four-satellite Disaster Monitoring Constellation (DMC) flown by Surrey Satellites Technology Limited (SSTL) currently provides medium GSD (32 m) full daily coverage of the Earth at a cost below that of a single traditional EO satellite mission [8]. Similarly, with a light-weight and compact TIR EO instrument, a medium GSD (325 m), medium NETD (< 0.5 K), but because of the nature of constellations, a low ground revisit time (2 –3 days) TIR data set will be capable of complementing the already existing DMC imaging products. This potential capability is denoted in Fig. 1 by the circle in the lower-left region of the diagram. While the utility of this data class is still largely unexplored, it would undoubtedly provide a unique service for those wishing to analyse trends or detect anomalous changes in the TIR characteristics of the Earth's surface or atmosphere.
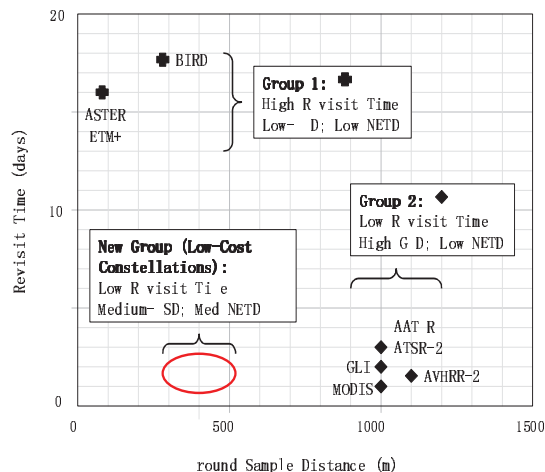

Fig. 1: Ground Revisit Time vs. GSD
for several major TIR EO missions [1-7]

In this study, the advantages of small, low-cost satellites have been used as a foundation for the development of a novel miniature TIR EO instrument. In the following sections, a preliminary mission analysis will be presented followed by the instrument concept and its expected performance.

2. MISSION DESIGN

In order to realise this new class of data, our TIR EO instrument needs to be small and light enough to fly on multiple platforms at an affordable cost. However, at the same time the instrument has to be powerful enough (GSD and NETD) to create useful data sets. In order to select the proper balance between these two factors (size/mass and performance), a trade space was bounded by two thresholds. The first threshold is defined by size, mass, and power limits enabling integration into the SSTL DMC imaging suite. The second threshold is defined by TIR EO performance parameters, namely GSD, NETD, and revisit time. The intercept of these two areas defines our trade space for instrument development.

2.1 Microsatellite size/mass/power thresholds

The key contributor to the uniqueness of this proposed TIR EO instrument are the severe mass and size constraints presented by the DMC micro-satellite platform. Although the trend for TIR EO instruments leverages recent advances in the miniaturization of infrared imaging technologies, very few proposed instruments have yet been taken to this extreme. The current limits taken by the TIR EO instrument include those set by DLR's 30 kg BIRD instrument [3] and those proposed by NASA and ESA with the use of uncooled micro-bolometer arrays [9-11]. Although these designs make it possible to fly high-performing TIR (and mid-wave IR) instruments on micro-class satellites (< 100 kg), they would easily consume the entire payload budget for a DMC micro-satellite. Whilst the flight of these instruments in micro-satellite constellations have potential to fill an important TIR EO niche, it is the focus of Surrey in this study to push TIR EO instrument miniaturization to yet another level. The reasons for doing this are as follows. First, by developing a radically small TIR EO instrument, it can more easily be integrated into the already existing DMC imaging suite. This includes capabilities in medium (32 metre GSD) to medium-high (4 metre) resolution visible and NIR EO. Also, since the TIR is a relatively new development area for Surrey, technological risks can be significantly reduced by starting simple and small much like the earlier development of its current generation of visible and NIR EO capabilities. By slowly introducing TIR to the DMC constellation, the market and utility can be tested

at a relatively low cost. Therefore, for this study, the following mass and size thresholds have been determined iteratively with the mission utility thresholds and the instrument design described in the next sections.

Baseline Boundary Conditions	Value
approx. weight	< 2-3 kg
approx. size (optics & detector)	< 2,000 cm^3
approx. power consumption	< 5 W

Tab. 1: Baseline constraints for the TIR imager

2.2 Mission utility thresholds

The second boundary for the trade space are defined by the acceptable levels of GSD and NETD, in light of the increases in revisit time brought by the constellation. Traditionally, spatial (GSD) and radiometric (NETD) resolution requirements for new TIR EO instruments result from an active dialogue and eventual compromise between the user community, who always seeks greater spatial, radiometric, and temporal resolution, and instrument design engineers who determine what is physically and economically feasible. This compromise has solidified over the years and both the user community and instrument developers have since grounded their processes to the capabilities of heritage systems. As a result, somewhat of a departure must be made to validate the new class of data enable by micro-satellite constellations.

Therefore, when evaluating the mission utility of adding a TIR band to DMC, the existing field of TIR requirements has been used as a starting point but has been adapted to exploit the advantages brought by small satellites (reducing costs of existing data sets or providing niche services currently ill-served). The advantages or niche provided by this type of data has been illustrated in Fig. 2. In the upper half of the figure, representative course spatial but high temporal data is compared with more precise spatial but low temporal data (group 1 in Fig. 1). Although the latter data set is much better suited at geo-locating TIR phenomena, the former is better at monitoring the migration of thermal events across the scene.

In the lower half of Fig. 2, course radiometric but high temporal data is compared with precise radiometric but low temporal data (again group 1). In this case, the latter data set is better at determining the surface temperature/emissivity characteristics of the scene. However, the former is much better suited to detect a brief change in scene temperature/ emissivity.

Geolocation of Thermal Event vs. Time

Earth Surface Temperature (K) vs. Time
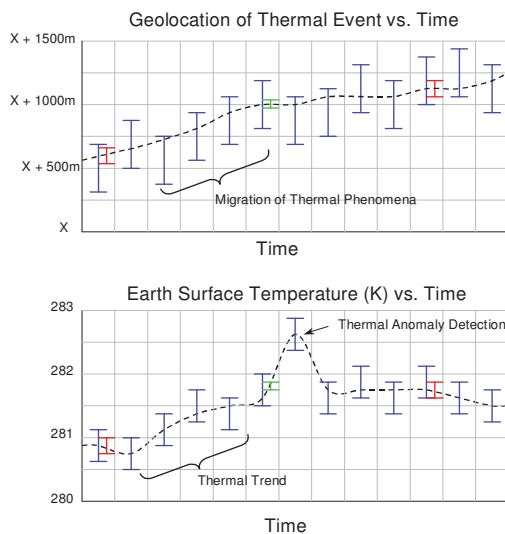
Fig. 2: Less precise TIR EO data
(spatially and radiometrically) becomes more useful
with decreased revisit time

Therefore, in defining suitable mission areas for this new class of compact TIR EO instrument for flight in multi-satellite constellations, two general mission areas were the focus: 1) **analysis of trends**, and 2) **detection of anomalous changes** in the spatial or radiometric characteristics of the TIR signature of the Earth's surface or atmosphere. Development of a sound set of mission applications for this new class of TIR EO data still requires a rigorous dialogue with the user community. However, using a 2003 ESA study (Thermal High-Resolution Earth Mapper - THEMA) reference [12], the following candidate mission applications have served as the starting point for this instrument development:

Mission Application	GSD	NETD	Revisit Time
Thermal Trend Analysis			
• Forest canopy temp	300		day
• Crop hydric stress	200	0.1– 0.3 K	day
• Volcanic plumes	200	0.1– 0.3 K	day
• Costal & marine	300	0.1– 0.3 K	day
Thermal Change Detection			
• forest fire detection	200	1.5-2.5K	1 h
• volcanic eruptions	50	1.5-2.5K	week

Tab. 2: Sample Mission application for
TIR EO micro-satellite constellations [12]

The THEMA study provides a good starting point because it represents a recent and thorough analysis of user requirements and the general acceptance by the TIR data users. Of special interest is forest fire detection, which, if used in conjunction with on-board

detection algorithms and autonomous ground user data transfer, would fill an important niche in the global fire detection community.

2.3 Trade study (size/mass vs. performance)

With the size/weight and utility objectives defined, the iterative generation of the remainder of the instrument's requirements was performed. During this process, trade-offs between performance (GSD, NETD, and revisit time) and estimated size, mass, and power requirements were made. For our instrument, NETD could be decreased by increasing the amount of scene energy available to the detector, i.e. lowering the f/#, increasing the spectral bandwidth, or employing time delayed integration (TDI). In the same way, spatial resolution and ground coverage could be increased or decreased by adjusting the imager focal length within the payload size limitations. The sub 8 - 12 μm wavebands in Tab. 3 have been chosen based on heritage TIR missions and the inevitable requirement for atmospheric correction, discriminating ground features, and customisation (e.g. utilizing a split window technique). Taking all these factors into account the following list of requirements was used for the baseline design.

Initial Requirement (selectable)	Value
Imaging mode	Staring array or pushbroom
GSD @ 700 km	325 m
Swath width	100 km (200 km for camera pair)
Candidate spectral channels	8-9, 10-11, 11-12, 8-14 μm
Spatial frequency	> 20 % Nadir MTF @ Nyquist Freq.
Temperature accuracy	< 0.5 K at 300 K

Tab. 3: Summary of requirements for TIR imager

2.4 Typical microsatellite mission

Given the fundamental limits encountered by a low-cost, compact imager, it's performance as a complement to a larger imaging suite becomes important. In this section a potential mission concept resulting from the integration on a 90 kg DMC-type micro-satellite will be briefly presented. Given the varied specifications required by the multiple owners of DMC, there are several different versions of the DMC spacecraft. However, the orbital characteristics are all essentially the same; Sun-synchronous with a local time of the ascending node at 10:00 am, at near 700 km altitude. This has been chosen so that between 4 and 8 spacecraft can provide daily coverage at the Equator with 300 – 600 km ground swaths. A typical DMC imager is composed of six push-broom CCD

sensors, configured in two banks of three (red, green and NIR), as part of an overall optical bench assembly. Two tri-axial vector magnetometers and four dual-axis sun-sensors are carried in order to determine the attitude of the spacecraft to better than ± 0.25 degrees, however control is relaxed at ±1 degree. For the addition of a TIR channel (also as an imager pair), the baseline spacecraft EO payload would most likely have the following characteristics:

Waveband	GSD	Swath Width
Visible (0.52 – 0.62 µm)	32 m	600 km
NIR (0.76 – 0.9 µm)	32 m	600 km
TIR (8 – 12 µm)	325 m	200 km

Tab. 4: Potential micro-satellite TIR imaging mission

The entire EO payload (3 imager pairs) would weigh less than 10 kg. While a wideband (8 - 12 µm), 325 m GSD instrument has been used in this example, the TIR channel for a real DMC mission would be customized to accommodate specific mission requirements.

3. INSTRUMENT DESIGN

3.1 Cooled vs. uncooled detector technology

The goal in detector selection has been to find candidate commercially available detector array that offer the best performance in terms of weight, size, power consumption, and cost. The TIR EO designer has a variety of cooled technologies to choose from, including ever-shrinking cryo-coolers that are increasingly more power efficient and relatively stable with regards to inducing micro-vibrations. However, in this study, we are looking for an order of magnitude decrease in mass–moving to approximately the 2-3 kg mass range–whilst still achieving reasonable mission utility. Cooled TIR technology may eventually become part of the DMC EO suite, but given reasons outlined in section 2.1, un-cooled detectors have become a practical first step to image in the TIR band.

3.2 Choices in un-cooled technology

In this survey the three main classes of un-cooled infrared technology (pyroelectric, thermoelectric, and resistive bolometer) were initially evaluated. The last class of un-cooled infrared technology, resistive bolometers, has recently been the most aggressively developed of the three for terrestrial applications. Resistive bolometers have been around for decades, but it has been the recent developments in MEMS and thin film technologies that has led to a surge in commercially available micro-bolometer arrays. These arrays are finding multiple markets in fire fighting,

security, and manufacturing, which encourages streamlined production processes and increasingly less expensive and better performing devices.

After examining over 32 models from 11 different manufacturers, we have initially settled on a French COTS 320 x 240 amorphous silicon micro-bolometer array on which to base our preliminary design. The array has a pixel pitch of 45 µm with an 80 percent fill factor. The detector response is reported to be 4 mV/K and the thermal time constant is 4 ms. The NETD is given as 120 mK with f/1 optics observing a 300 K target. In addition, the array comes integrated with a thermally stabilized Peltier cooler, and read-out integrated circuit (described in section 3.4). The values for peak responsivity ($\Re$) and rms noise (V_N) were not directly specified but were calculated to be approximately 7×10^6 V/W and 480 µV respectively from the specified parameters. These values are consistent with data found in other previously published reports. [11]

The key rationale this array was chosen was that it is fairly representative of the state of the art and is readily available within the European academic community. However, the nature of rapid micro-satellite development times supports the insertion of any technology that is deemed appropriate during the initial design phase. For subsequent TIR imager designs, other COTS detector arrays may be selected using the best fit at the time.

3.3 Initial optics design

The final optical design will not be defined until after the laboratory test phase of our development cycle. However, a preliminary concept has been laid out given the required point spread function (PSF) and modulation transfer function (MTF) derived from the baseline requirements. For the bench-top prototype, the most liberal requirements were chosen to facilitate a low development cost and a short development timeline. The resultant baseline design is f/1.2 refractive lens triplet with a focal length of 100 mm.

3.4 Initial electronics design

At the micro-bolometer pixel level, absorbed incident radiation causes a change in pixel temperature, which, in the case of semiconducting bolometric materials, reduces its electrical resistance. Since the pixel is pulse biased with a set voltage, the resultant change in current signal can be measured by the detector read out integrated circuit (ROIC), which is part of the COTS detector package. After a thermal scene is 'imaged' on the array, the respective signal currents are reduced by a dark pixel current and then integrated into a voltage

signal row by row at the bottom of each array column (ripple operation). In turn, all 76,800 pixels are read out as a 5 MHz analogue video signal resulting in a 50 Hz frame rate. One of the key advantages of using a COTS detector is the ease of electrical interfacing via the ROIC. The video output from the ROIC is similar to that found on some of our current imager systems, and so we had made use of our design heritage for image acquisition, storage and downloading.

After leaving the detector ROIC, the analogue video signal enters the SSTL engineered electronics. The video signal is first digitised to an 12-bit digital stream and then read into a solid-state data-recorder (SSDR). The data is then held until ready for transmission to Earth under the control of a field programmable gate array (FPGA), which links the SSDR to a dedicated downlink. The FPGA also contains all the sequencing and timing logic for system, as well as all the control signals needed to operate the imager under the various data collection scenarios. The command and control of the FPGA is performed by a microcontroller. The microcontroller sends and receives telecommands and telemetry though Control Area Network (CAN) packets from other on-board controllers. It can also provide on-board image processing such as automatic feature detection and data-compression. The downlink speed will depend on the particular host satellite. Typical rates for microsatellites range from 9.6 kbps to a few Mbps.

3.5 Calibration

One of the key challenges in flying TIR imagers on very small spacecraft is that of instrument calibration. In order to accurately measure ground feature temperatures, reference blackbodies are typically temporarily inserted within the imager field of view to calibrate the effects of inevitable drifts in the imager parameters. Standard practice with heritage systems is to utilize one cold and one hot blackbody to accurately reference the radiometer prior to taking each image. On larger systems, this has been done with the same steering mirror used for image scanning in a whiskbroom configuration. In smaller systems, mechanical arms, mirrors, or paddles are used. In most cases, cold space (3 K) is used as the required cold body and the hot body is on-board the spacecraft bus.

For our system, calibration schemes can complicate what has been so far a relatively simple and low-cost design. For some mission areas such as those focusing on thermal contrast instead of exact radiometric measurements, on-board calibration may not be required so a non-calibrated system is definitely a consideration for this design. However, one of the advantages of a small, nimble spacecraft is its ability to

manoeuvre. The final calibration method is to be determined but heavy emphasis will be given to the use of manoeuvre (spacecraft pan towards cold space) or settling strictly on relative variation mapping with potential cross-calibration with other instruments (such as AATSR). However, consideration will be given to on-board calibration when mission requirements dictate.

4. EXPECTED PERFORMANCE

Before committing to the expense of prototyping the instrument, it is important to examine a realistic prediction of on-orbit radiometric performance. In the following section, the expected performance will be examined by looking at the expected signal to noise ratio (SNR) as well as the noise equivalent temperature difference (NETD) of a nominal Earth scene. In order to evaluate the SNR for various mission scenarios, the following definition was applied: [13]

$$SNR = \frac{P_I}{P_N} \qquad (1)$$

where P_I is the collected radiant power at the detector pixel and P_N is the detector noise equivalent power (radiant power incident upon a pixel which gives rise to a signal equal to the rms pixel noise within the system bandwidth). In micro-bolometers, there are four primary sources of noise: Johnson noise, 1/f power law noise, temperature fluctuation noise, and background fluctuation noise. For our detector array, the combined noise contributed by both the micro-bolometer detector and the electronics was calculated to be approximately 1.4 mV. Putting P_I in terms of scene temperature/emissivity and taking into account atmospheric and optical losses as well as detector efficiency, Eq. 2 has been derived:

$$SNR = \frac{A_D}{4(f/\#)^2 V_N} \int_{\Delta\lambda} W(\lambda)\Re(\lambda)\tau_O(\lambda)\tau_A(\lambda)d\lambda \quad (2)$$

where A_D is the detector area, $\Re$ is the detector responsivity in volts per incident watt, τ_O and τ_A are the imager optical and atmospheric transmissions respectively, and W is the thermal irradiance of the ground scene (W/m^2). Since the last four terms are wavelength dependent, their combined effect is integrated across the selected waveband.

In order to take advantage of the 2-D nature of the detector array and the scanning nature of the orbiting spacecraft, time delay integration (TDI) has been

factored into the design. The use of TDI with a 2-D micro-bolometer array in space was successfully demonstrated in 1997 by Goddard Space Flight Center on their Infrared Spectral Imaging Radiometer (ISIR) [9]. With TDI, successive rows of imagery are averaged as they pass over the same scene (see Fig. 3). If applied correctly, matching successive rows exactly, this process has the potential to increase the SNR by the square of the number of rows used.
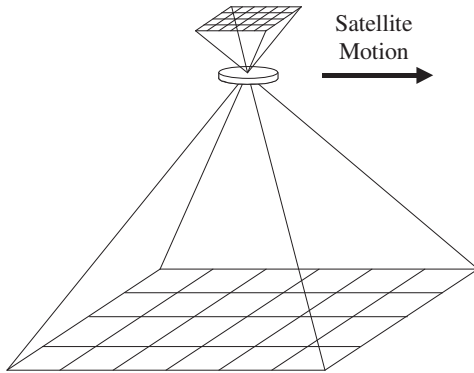

Fig. 3: Application of the 2-D array to
perform time-delayed integration (TDI)

So, returning to Eq. 2, Planck's curve for a 300K blackbody was combined with John Hopkins University emissivity data (found in the ASTER Spectral Library version 1.2) [14] and the MODTRAN computer model [15] to model Earth scene radiance across the thermal infrared (8 – 12 μm). Assuming a 75% optical transmission, f/1.2 optics, 45 μm pixel pitch and 80 % fill factor, 1.4 mV of detector and electronics noise, a detector responsivity modelled on the vendor published spectral response and peaking at 7×10^6 V/W, and 50 of the 240 available pixel rows used for TDI, the SNR values in Tab. 6 were calculated for a 300 K ground scene.

Waveband	SNR (TDI 50)
8 – 9 μm	106
10 – 11 μm	153
11 – 12 μm	132
8 – 12 μm	495

Tab. 5: SNR for various thermal imaging wavebands

While these calculations are reassuring, they assume the scene irradiance is much higher than the background. Therefore, it is important to examine the

noise equivalent temperature difference (NETD). The NETD is one of the most important figures of merit in any thermal imaging system. In addition, the vendor usually specifies a baseline NETD so it is straightforward to compare candidate detectors. However, NETD is a function of the instrument configuration so an understanding of the vendor's measurements conditions and their relationship with that of a space-borne application is important. Since NETD can be defined as the difference in temperature between two blackbodies of large lateral extent that, when viewed by a thermal imaging system, causes a change in SNR of unity, the following expression can be derived from Eq. 2. This is done by differentiating with respect to temperature, and setting SNR to one.

$$NETD = \frac{4(f/\#)^2 V_N}{A_D}\left(\int\limits_{\Delta\lambda}\left(\frac{\Delta W(\lambda)}{\Delta T}\right)\tau_O(\lambda)\tau_A(\lambda)\Re(\lambda)d\lambda\right)^{-1} \quad (3)$$

where V_N, A_D, τ_O, τ_A, and $\Re$ are the same as previously defined. In (3), $(\Delta W(\lambda)/\Delta T)$ represents the change with respect to temperature in the power per unit area emitted by a blackbody at temperature, T, measured with the spectral bandwidth $\Delta\lambda$. In a laboratory environment, at $T = 300$ K and across 8 – 12 μm, $(\Delta W(\lambda)/\Delta T) = 2.59$ W m^{-2} K^{-1} which, assuming no atmospheric losses, corresponds to the vendor specified NETD of 120 mK. However, we are interested in NETD as it relates to a thermal Earth scene, and so atmospheric effects, as well as sub divided wavebands are factored into (3). Taking into account the TDI of 50 pixel rows, the results are listed in Tab. 6:

Waveband	NETD (TDI 50)
8 – 9 μm	0.50 K
10 – 11 μm	0.47 K
11 – 12 μm	0.53 K
8 – 12 μm	0.12 K

Tab. 6: NETD for various thermal imaging wavebands

The authors realise the limited applicability of simple performance calculations such as we have presented in this paper to real world space systems. The decision to commit to a given technology and ultimately a detailed spacecraft instrument design is not one to take lightly, given the heavy investments and risks required. However, the preliminary SNR and NETD calculations show promise that a low-cost and compact approach is feasible. Even though the requirements listed in section 2.3 were loosely and liberally defined, it appears we can well satisfy them. In order to confirm our theoretical findings, hardware testing is planned over the next year at Surrey.

5. ASSESSMENT: EO AND UN-COOLED TECHNOLOGY

Given the radiometric performance of today's un-cooled infrared detector technology, it has become apparent that they are a valid approach for some TIR EO applications. However, un-cooled technology still holds some basic fundamental limits, which must be realized and accepted before using this approach. One of these limitations is the generally low radiometric response compared to cooled technology. As a result, un-cooled detectors require relatively fast optics. This becomes a major issue when trying to achieve GSDs less than about 250 m from a very small satellite where entrance apertures are limited to approximately 15 to 20 cm or less. Also, a low responsivity means that spectral bandwidths can only be reduced to a certain point. When trying to distinguish scene spectra, a large bandwidth can prove troublesome. For example, reducing the spectral bandwidth from 4 to 1 μm reduces amount of available scene flux by ¾. For systems where SNR is marginal, this becomes significant.

However, despite these fundamental limits, the advantages of un-cooled technology make them attractive for micro-satellite developers. In our case, the step to relatively bulky, expensive, and power hungry cryogenically cooled detectors is significant, especially when a potential alternative has yet to be fully discounted. Put simply, the low cost and compact state of commercial un-cooled technology can be the key enabling technology to the integration of a TIR channel(s) in a DMC-like micro-satellite EO constellation. In this, it is not a question of cooled versus un-cooled but rather, un-cooled or nothing. The ultimate utility for un-cooled TIR detector technology lies in low-cost and highly specialized niche mission areas that benefit greatly from the high temporal resolution offered by satellite constellations. As outlined earlier in this paper, this new class of mission areas is expected to grow once a low-cost capability has been established.

Although the un-cooled detector industry has just become ripe for EO mission evaluation, it will only become more so in the future, as the commercial industry continues to improve their products. Some of the developments already coming to market include pitch reduction down to 25 μm and array size growth to 640 x 480. This will enable even greater GSD and swath for the same size optics. In addition, reported NETDs are nearing 20 mK and lower. The commercial market for terrestrial TIR cameras has grown tremendously and the small EO satellite stands to profit from this if potential users are prepared to see the advantages.

6. CONCLUSION

In conclusion, the Surrey Space Centre believes the commercial un-cooled infrared detector array market holds promise for low-cost EO in the TIR. Over the next year, we will be characterizing and testing an imager prototype with the aim of creating novel design options for EO. In the imager development, special emphasis will be given to potential operating in the MWIR, dual channel imaging on the same detector array, and the forest fire detection mission area by parallel development of on-board detection algorithms and autonomous ground user data transfer. It is expected that the same principles applied to the development of low-cost alternatives to the UV, visible, and NIR can be applied to the TIR with fruitful results.

7. ACKNOWLEDGEMENTS

8. DISCLAIMER

The views expressed in this article are those of the authors and do not reflect the official policy or position of the United States Air Force, Department of Defence, or the U.S. Government.

9. REFERENCES

1. AATSR homepage (29 Jan 04):
http://envisat.esa.int/dataproducts/aatsr/

2. MODIS homepage (29 Jan 04):
http://modis.gsfc.nasa.gov/

3. DLR BIRD homepage (29 Jan 04):
http://spacesensors.dlr.de/SE/bird/

4. NASA ETM+ data page (29 Jan 04):
http://eospso.gsfc.nasa.gov/eos_homepage/mission_profiles/instruments/ETM.php

5. ASTER homepage (29 Jan 04):
http://asterweb.jpl.nasa.gov/

6. ADEOS GLI Webpage (29 Jan 04):
http://adeos2.hq.nasda.go.jp/shosai_gli_e.htm

7. AVHRR-2 Webpage (29 Jan 04):
http://www.eumetsat.de/

8. da Silva Curiel, Alex, et. al., "First Results from the Distaster Monitoring Constellation (DMC)", *presented at the 2003 IAF Congress*, Bremman, Germany, paper IAA-B4-1302.

9. Spinhirne, James D. et. al., "Preliminary Spacecraft Results from the Uncooled ISIR on Shuttle Mission STS-85", http://isir.gsfc.nasa.gov.

10. Saint-Pé, Olivier, et. al., "Study of an uncooled focal plane array for thermal observation for the Earth", *Proceedings of SPIE Vol. 3436*, pp. 593 – 604, 1998.

11. Geoffray, Hervé, et. al., "Measured performance of a low cost thermal infrared pushbroom camera based on uncooled microbolometer FPA for space applications", *Proceedings of SPIE Vol. 4540*, pp. 298 – 308, 2001.

12. Coppo, Peter, et. al., "Requirements and Design of a Thermal High-Resolution Earth Mapper (THEMA) Based on Uncooled Detectors", *Proceedings of SPIE Vol. 4881*, pp. 531 – 542, 2003.

13. Kruse, Paul W., *Uncooled Thermal Imaging, Arrays, Systems, and Applications*, SPIE Press, 2001.

14. ASTER Spectral Library Version 1.2, http://speclib.jpl.nasa.gov, JPL, California Institute of Technology, 1998.

15. MODTRAN 3.7 Version 1.0, Air Force Research Laboratory, 11 Nov 1997.